sciendo

**ARTICIAL SATELLITES, Vol. 58, No. 3 – 2023**
**DOI: 10.2478/arsa-2023-0008**

# ANALYSIS OF THE ITSG-GRACE DAILY MODELS IN THE DETERMINATION OF POLAR MOTION EXCITATION FUNCTION

Aleksander PARTYKA[1], Jolanta NASTULA[1], Justyna ŚLIWIŃSKA[1], Tomasz KUR[1], Małgorzata WIŃSKA[2]

[1] Centrum Badań Kosmicznych Polskiej Akademii Nauk, Warsaw, Poland
[2] Warsaw University of Technology, Faculty of Civil Engineering, Warsaw, Poland

e-mails: apartyka@cbk.waw.pl, nastula@cbk.waw.pl, jsliwinska@cbk.waw.pl, tkur@cbk.waw.pl, malgorzata.winska@pw.edu.pl

**ABSTRACT.** The main aim of this study is to evaluate the usefulness of Institute of Geodesy at Graz University of Technology (ITSG) daily gravity field models in the determination of hydrological angular momentum (HAM) at nonseasonal time scales. We compared the equatorial components ($\chi_1$ and $\chi_2$) of HAM calculated with the ITSG daily gravity field models (ITSG-Gravity Recovery and Climate Experiment [ITSG-GRACE] 2016 and ITSG-GRACE 2018) with HAM and sea-level angular momentum (SLAM) from hydrological land surface discharge model (LSDM) and the hydrological signal in the polar motion excitation (known as geodetic residuals [GAO]). Data from ITSG have a daily temporal resolution and allow us to determine oscillations with higher frequencies than the more commonly used monthly data. We limited our study to the period between 2004 and 2011 because of the gaps in GRACE observations before and after this period. We evaluated HAM obtained from ITSG GRACE models in spectral and time domains and determined the amplitude spectra of the analyzed series in the spectral range from 2 to 120 days. Our analyses confirm the existence of a sub-monthly signal in the HAM series determined from ITSG daily data. We observed a similar signal in LSDM-based HAM, but with notably weaker amplitudes. We also observed common peaks around 14 days in the amplitude spectra for the GAO- and ITSG-based series, which may be related to the Earth's tides. ITSG daily gravity field models can be useful to determine the equatorial components of HAM at nonseasonal time scales.

**Keywords:** GRACE, hydrological angular momentum, Earth rotation, polar motion excitation

## 1. INTRODUCTION

Mass redistributions, along with movements of the solid part of the Earth, such as tectonic plate movements and earthquakes, cause changes in the Earth's rotational motion. The motion of the Earth's axis of rotation relative to its surface, namely, polar motion (PM), is caused mainly by the global mass distribution of the Earth's atmosphere, ocean, land hydrosphere, and cryosphere (Lambeck, 1980; Gross, 2015; Bizouard, 2020).

Disturbance of the Earth's PM resulting from the changes in mass distribution of its surficial fluid layers (atmosphere, ocean, and continental hydrosphere) can be described with effective angular momentum (EAM) functions, being a modified linearized Liouville equation

©The Author(s). This is an open-access article distributed under the terms of the Creative Commons Attribution License (CC BY 4.0, https://creativecommons.org/licenses/by/4.0/), which permits use, distribution, and reproduction in any medium, provided that the Article is properly cited.

expressed as two equatorial components ($\chi_1$, $\chi_2$) and one axial component ($\chi_3$), and can be derived from observational data (Munk and MacDonald, 1960; Brzeziński, 1992). The $\chi_1$ and $\chi_2$ components of the EAM function describe the PM excitation caused by perturbing forces, while $\chi_3$ is related to the day-length fluctuations caused by these forces. The EAM function, depending on the factor disturbing it, is expressed as atmospheric angular momentum (AAM), oceanic angular momentum (OAM), or hydrological angular momentum (HAM). Analyses of the sources of terrestrial hydrological signals in PM excitation indicate that HAM can explain some of the changes in PM excitation after the effects of AAM and OAM are removed (Chen and Wilson, 2005; Jin et al., 2010; Śliwińska et al., 2022). HAM can be estimated from global models of the continental hydrosphere, measurements of changes in the Earth's gravitational field, and climate models (Seoane et al., 2011; Meyrath and van Dam, 2016; Göttl, 2018).

Previous studies have shown that hydrological excitation is important in determining PM excitation (Dobslaw et al., 2010; Meyrath and van Dam, 2016). The impact of HAM signals on PM excitation from changes in mass distribution has been little studied than the impact of AAM and OAM signals, particularly if we consider oscillations with a period shorter than annual (Chen et al., 2000; Nastula et al., 2019). It has previously been shown that, at seasonal time scales, PM excitations from geophysical fluids (i.e., atmosphere, ocean, and hydrosphere) agree well with geodetic observations of PM in the $\chi_2$ component (Göttl et al., 2018, Chen et al., 2012). For the $\chi_1$ component, considerable discrepancies were shown between the PM excitations and the geodetic observations (Seoane et al., 2011; Chen et al., 2012; Wińska et al., 2017).

Since the Gravity Recovery and Climate Experiment (GRACE) mission began in 2002, scientific teams at the Center for Space Research (CSR, Austin, USA), GeoForschungsZentrum (GFZ, Potsdam, Germany), and Jet Propulsion Laboratory (JPL, Pasadena, USA) have been providing GRACE-based monthly gravity field solutions (Tapley, 2004). These data can be used to interpret PM excitation perturbations caused by changes in the mass distribution of continental hydrosphere, focusing on different oscillations and periods. Compared with HAM from geophysical models of the hydrosphere, GRACE-based HAM has been shown to be more consistent with the hydrological signal in PM excitation obtained from geodetic observations (Chen et al., 2012; Nastula et al., 2019; Śliwińska et al., 2020; Wińska et al., 2017). In addition to monthly gravity field solutions, the Institute of Geodesy at Graz University of Technology (ITSG) also produces daily solutions, providing the only available GRACE-based data at daily resolution (Kurtenbach et al., 2012). Daily solutions based on the GRACE data have not yet been considered for tackling the components of HAM.

The main aim of the current study is to assess the usefulness of the daily gravity field models from the GRACE mission delivered by the ITSG as ITSG-Grace2016 (abbreviated here as ITSG 2016) and ITSG-Grace2018 (abbreviated here as ITSG 2018) to determine the equatorial components ($\chi_1$ and $\chi_2$) of HAM. These are compared with HAM derived from the hydrological signal in geodetically observed PM excitation (called geodetic residuals [GAO]) and HAM based on hydrological land surface discharge model (LSDM). We analyzed HAM at daily temporal resolution, which allows us to determine oscillations with higher frequencies than the more commonly used monthly data. This provides an opportunity to investigate the existence of a sub-monthly signal in the HAM data.

The structure of this paper is as follows. Section 2 describes data and methodology: section 2.1 presents the ITSG 2016 and ITSG 2018 daily gravity field models and describes the method of computing HAM excitation from the ITSG solutions, section 2.2 includes characteristics of the geodetic residuals and sources of the data, section 2.3 describes features of HAM based on LSDM, and section 2.4 explains the steps of the calculations performed.

Section 3 presents the results of our study: section 3.1 shows the time series comparison, section 3.2 presents amplitude spectra of the series, and section 3.3 includes validation of series with root mean square error (RMSE), relative explained variance ($Var_{exp}$), and correlations. Finally, section 4 provides a discussion of the results and presents the conclusions of our study.

## 2. DATA

### 2.1. ITSG daily gravity field models

Daily ITSG 2016 and ITSG 2018 gravity models were used to calculate $\chi_1$ and $\chi_2$ of HAM (Table 1). We selected these two models because of the identical availability of their data during our chosen period, giving rise to the possibility of comparing them. These models are characterized by an increase in temporal resolution to 1 day compared with more common monthly data. The increase in resolution was made possible by the application of a Kalman smoother estimation procedure (Kurtenbach et al., 2012).

ITSG 2016 and ITSG 2018 differ in terms of the background models used to produce them, for example, the ocean tide, pole tide, ocean pole tide, atmospheric tides, atmosphere and ocean de-aliasing, and sub-monthly continental hydrology (Table 1) (Mayer-Gürr et al., 2016, 2018). ITSG 2018 is the most recent realization of the GRACE solution provided by ITSG.

The ITSG data used for our calculations were taken from Graz University of Technology (TU Graz) resources (http://ftp.tugraz.at/outgoing/ITSG/GRACE/, accessed on 25.01.2022).

**Table 1.** Models used to produce the ITSG 2016 and ITSG 2018 series

| | **ITSG 2016** | **ITSG 2018** |
|---|---|---|
| Earth rotation | IERS 2010 | IERS 2010 |
| Moon, sun, and planets ephemerides | JPL DE421 | JPL DE421 |
| Earth tide | IERS 2010 | IERS 2010 |
| Ocean tide | EOT11a | FES2014b, co-estimated |
| Pole tide | IERS 2010 (constant mean pole) | IERS 2010 (linear mean pole) |
| Ocean pole tide | Desai 2004 (IERS 2010) | Desai 2004 (IERS 2010, linear mean pole) |
| Atmospheric tides (S1, S2) | van Dam, Ray (2010) | AOD1B RL06 |
| Atmosphere and ocean de-aliasing | AOD1B RL05 | AOD1B RL06 |
| Relativistic corrections | IERS 2010 | IERS 2010 |
| Permanent tidal deformation | Included (zero tide) | Included (zero tide) |

Based on information from TU Graz website (https://www.tugraz.at/institute/ifg/downloads/gravity-field-models/, accessed on 25.01.2022)

The $\chi_1$, $\chi_2$ components of HAM excitation were calculated from the ITSG solutions based on their proportionality to changes in the coefficients $\Delta C_{21}$, $\Delta S_{21}$ of the geopotential (Gross, 2015):

$$\chi_1 = -\sqrt{\frac{5}{3}} \cdot \frac{1.608 \cdot R_e^2 \cdot M}{C - A'} \Delta C_{21} \quad (1)$$

$$\chi_2 = -\sqrt{\frac{5}{3}} \cdot \frac{1.608 \cdot R_e^2 \cdot M}{C - A'} \Delta S_{21} \quad (2)$$

where $R_e$ is the Earth's mean radius; M is the Earth's mean mass; A, B, and C are the principal moments of inertia for Earth ($A = 8.0101 \times 10^{37}$ kg·m$^2$, $B = 8.0103 \times 10^{37}$ kg·m$^2$, $C = 8.0365 \times 10^{37}$ kg·m$^2$); $A' = (A + B)/2$ is an average of the equatorial principal moments of inertia; and $\Delta C_{21}$, $\Delta S_{21}$ are the normalized spherical harmonic coefficients of the gravity field.

In the $\Delta C_{21}$, $\Delta S_{21}$ coefficients used in our study, the impact of atmospheric and oceanic nontidal mass variations was removed using GRACE Atmosphere and Ocean De-Aliasing Level-1B (AOD1B) data provided by GFZ. Consequently, GRACE-based HAM series included not only signals from the continental hydrosphere, but also some contributions from glacial isostatic adjustment (GIA) and barystatic sea-level variations resulting from inflow of water from land into oceans (so-called sea-level angular momentum [SLAM]). Nevertheless, GIA should affect only trends in PM excitation series, which are not analyzed in our study. To keep the highest consistency between GRACE-based HAM and HAM computed from hydrological models, one should add the contribution of SLAM to the series calculated from the models.

### 2.2. Geodetic residuals

The HAM series were evaluated based on comparison with the geodetic residuals, which represent the difference between geodetic angular momentum (GAM) obtained from precisely measured pole coordinates and the sum of AAM and OAM derived from geophysical models as follows:

$$\mathrm{GAO} = \mathrm{GAM} - \mathrm{AAM} - \mathrm{OAM} \quad (3)$$

GAO reflects mainly the impact of the land hydrosphere on PM excitation, but similar to HAM obtained from GRACE $\Delta C_{21}$, $\Delta S_{21}$ coefficients, it also includes SLAM and GIA signals.

The following data sets were used to calculate GAO:

- $\chi_1$ and $\chi_2$ equatorial components of the GAM series—EOP 14 C04 (IAU2000A), derived from the International Earth Rotation and Reference System Services (IERS) (https://www.iers.org/IERS/EN/DataProducts/EarthOrientationData/eop.html, accessed on 25.01.2022), available at a temporal resolution of 24 h;
- $\chi_1$ and $\chi_2$ equatorial components of the AAM series provided by GFZ and based on the European Centre for Medium-Range Weather Forecasts (ECMWF) model, available at a temporal resolution of 3 h (data available at http://rz-vm115.gfz-potsdam.de:8080/repository, accessed on 25.01.2022). The current AAM version provided by GFZ is consistent with GRACE AOD1B RL06 (AOD1B Release-6) data;
- $\chi_1$ and $\chi_2$ equatorial components of the OAM series provided by GFZ and based on the Max Planck Institute Ocean Model (MPIOM), available at a temporal resolution of 3 h (data available at http://rz-vm115.gfz-potsdam.de:8080/repository, accessed on

25.01.2022). The current OAM version provided by GFZ is consistent with GRACE AOD1B RL06 data.

### 2.3. LSDM-based series

ITSG-based series were compared with the sum of HAM and SLAM based on the LSDM hydrological model. The LSDM model was processed with the atmospheric and oceanic data from the ECMWF and MPIOM models, respectively (Dill et al., 2008). HAM based on LSDM was calculated by GFZ from terrestrial water storage and included the representation of soil moisture, shallow groundwater, snow coverage, and surface water stored in rivers and lakes. SLAM was calculated by GFZ on the basis of the spatially variable sea-level variations as inferred from globally integrating atmospheric and terrestrial masses in LSDM and ECMWF with consideration of self-attraction (Dobslaw and Dill, 2018). Global mass conservation was maintained in the AAM, OAM, HAM, and SLAM series produced by GFZ. The HAM and SLAM series used in our study were taken from GFZ resources (http://rz-vm115.gfz-potsdam.de:8080/repository, accessed on 25.01.2022).

## 3. METHODOLOGY

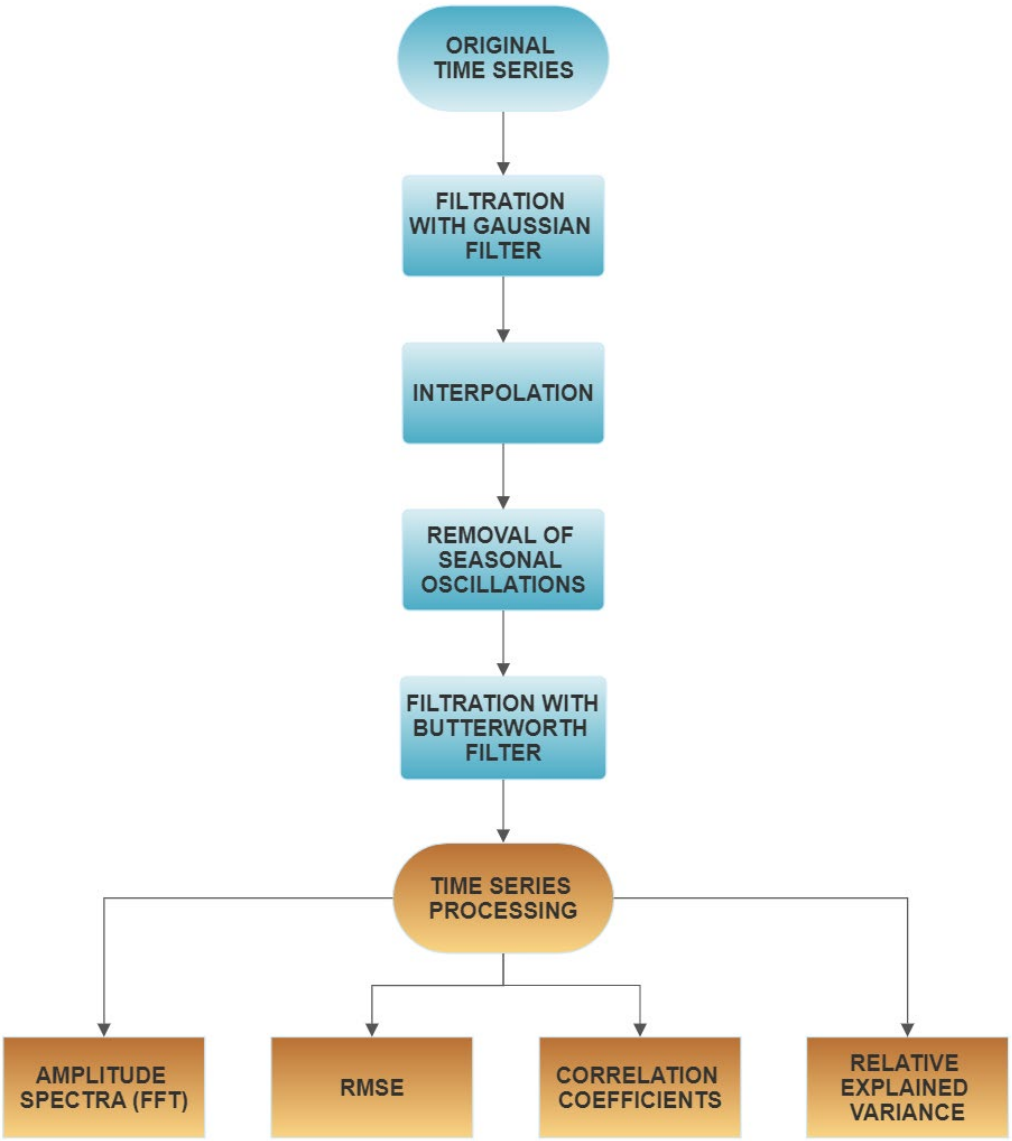


**Figure 1.** Methodology flowchart, which shows all the calculation steps

Our calculations and analyses were performed according to the following steps (Figure 1):

- application of a Gaussian filter with full width at half maximum (FWHM) equal to 2 to remove oscillations with periods shorter than 1 day (because the data we used have temporal resolution from 3 h to 1 day);
- interpolation of all time series to the same moments of time in order to obtain uniform data;
- removal of annual, semiannual, and terannual oscillations from the time series in order to analyze nonseasonal variations; this was done by fitting the second-order polynomial and sum of sinusoids with periods of a year, half a year, and a third of a year to the series;
- application of a fourth-order Butterworth filter with bandpass from 4 days to 120 days to the series in order to narrow our analysis to oscillations with periods below 120 days;
- use of fast Fourier transform to calculate the amplitude spectra of the series; and
- evaluation of ITSG-based HAM and HAM + SLAM by calculating RMSE, $\mathrm{Var}_{\mathrm{exp}}$, and correlation coefficients with GAO as a reference.

$\mathrm{Var}_{\mathrm{exp}}$ describes the variance compatibility between the reference series ($r$) and the evaluated series ($e$):

$$\mathrm{Var}_{\mathrm{exp}} = \left(\frac{\mathrm{Var}^{(r)} - \mathrm{Var}^{(r-e)}}{\mathrm{Var}^{(r)}}\right) 100\% \quad (4)$$

where $\mathrm{Var}^{(r)}$ is the variance of the reference series (GAO) and $\mathrm{Var}^{(r-e)}$ is the variance of difference between the reference series (GAO) and the evaluated series (ITSG 2016, ITSG 2018, or HAM + SLAM).

## 4. RESULTS

### 4.1. Time series comparison

Figure 2 shows that the GAO series has the highest amplitude and the ITSG-based series have considerably lower amplitudes than the GAO series. However, it is worth highlighting that the amplitudes of the ITSG-based series are clearly higher than those of the HAM + SLAM series. We can also see in Figure 2 that the ITSG 2016-based series has higher amplitudes than the ITSG 2018-based series. This is confirmed by the statistics shown in Table 2, which include standard deviation (STD), minimum (min), and maximum (max) values for the ITSG-based series, HAM + SLAM, and GAO. The ITSG 2016-based series has higher STD, higher maximum, and lower minimum values than the ITSG 2018-based series. This shows that the ITSG 2016-based series is closer to GAO than the ITSG 2018-based series in terms of time series variability.

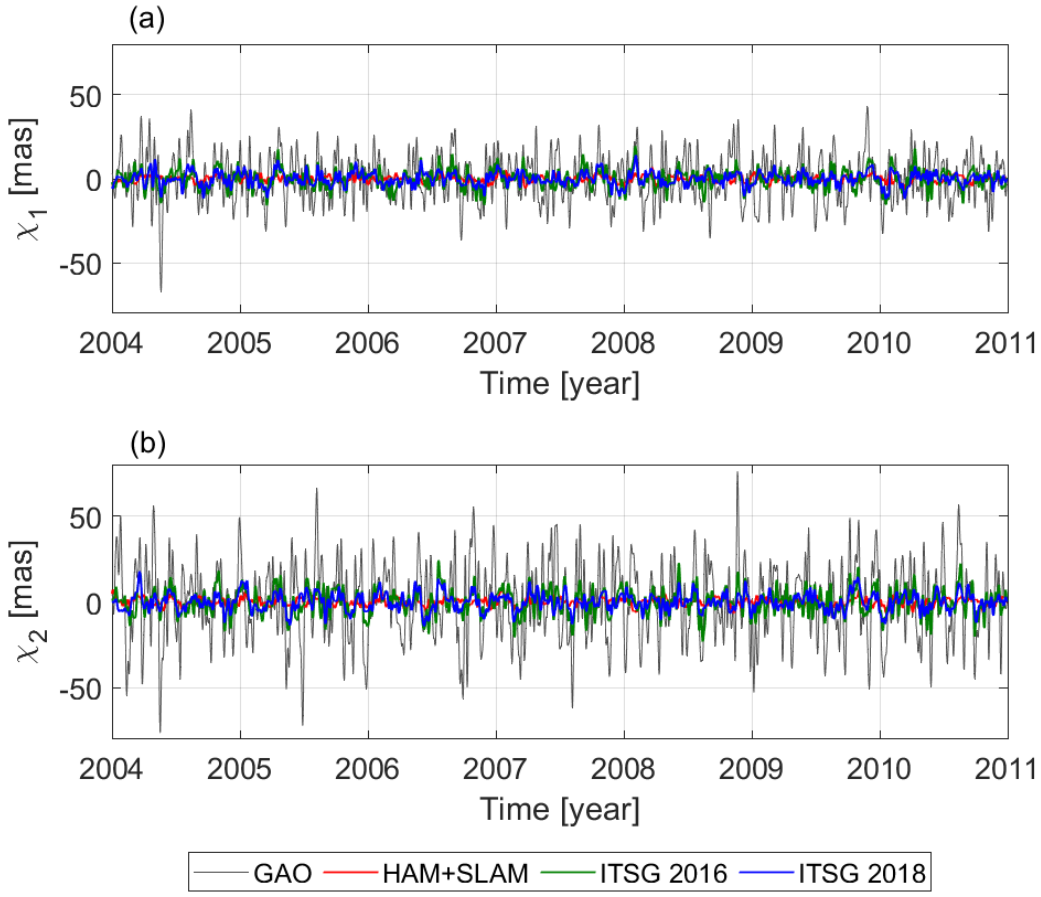


**Figure 2.** Comparison of the (a) $\chi_1$ and (b) $\chi_2$ components of nonseasonal series of GAO, HAM + SLAM, and HAM obtained from ITSG 2016 and ITSG 2018

**Table 2.** Comparison of STD, min, and max values from $\chi_1$ and $\chi_2$ nonseasonal series of GAO, HAM + SLAM, and HAM obtained from ITSG 2016 and ITSG 2018

| | **STD [mas]** | | **Min [mas]** | | **Max [mas]** | |
|---|---|---|---|---|---|---|
| **Series** | $\chi_1$ | $\chi_2$ | $\chi_1$ | $\chi_2$ | $\chi_1$ | $\chi_2$ |
| ITSG 2016 | 5.48 | 7.28 | −15.91 | −23.15 | 19.46 | 24.25 |
| ITSG 2018 | 3.90 | 5.05 | −12.04 | −14.11 | 14.03 | 17.84 |
| GAO | 13.71 | 21.76 | −67.01 | −76.18 | 42.90 | 76.10 |
| HAM + SLAM | 1.99 | 2.24 | −6.65 | −7.38 | 6.68 | 7.18 |

### 4.2. Amplitude spectra

Amplitude spectra of all considered series are plotted in Figures 3 and 4. In addition, Figures A1 and A2 of the Appendix show the same spectra, but with GAO excluded for better visibility.

Figure 3 presents the amplitude spectra of all series, which were computed for the periods between 20 and 120 days (Figure 3a and b for $\chi_1$ and $\chi_2$, respectively). Figure 4 focuses on the period between 2 and 20 days for better visibility of oscillations with shorter periods (Figure

4a and b for $\chi_1$ and $\chi_2$, respectively). Figure 3 shows that the GAO spectrum has the highest amplitudes and the HAM + SLAM series has the lowest amplitude, well below that of the other series. The ITSG-based series have several peaks in common with the GAO series. In $\chi_1$, the common peaks are found at 32.78 days, 98.34 days, and around 61 days (60.88 days for GAO, 62.37 days for ITSG). In $\chi_2$, the common peaks are found at 56.82 and 77.48 days.

Figure 4 shows the common peaks for ITSG 2016 and GAO around Day 14. For $\chi_1$, the peaks are at 13.67 days in GAO and 13.74 days in ITSG 2016. For $\chi_2$, the peaks are at 13.67 days in GAO and 13.53 days in ITSG 2016. These peaks may be related to the Earth's tide as they are positioned very close to the value of fortnightly ocean lunar tide with a period of 13.66 days. This value equals half of the Moon's declination changes with a period of 27.33 days (Bizouard, 2020; Sidorenkov, 2009).

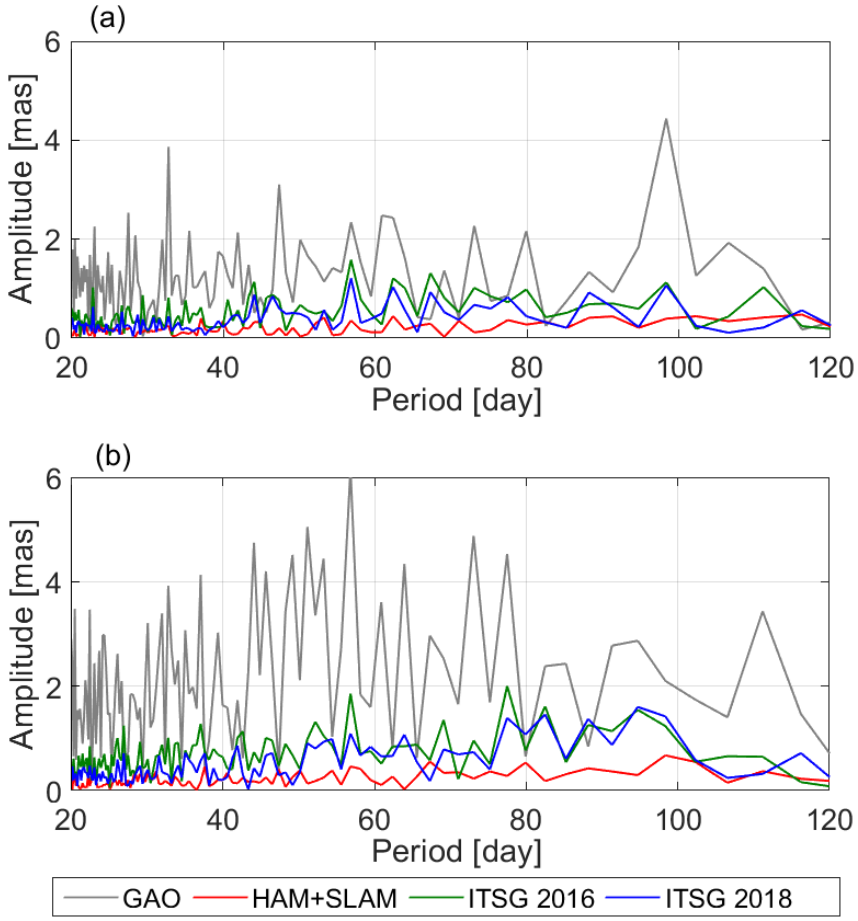


**Figure 3**. Comparison of (a) $\chi_1$ and (b) $\chi_2$ amplitude spectra series of GAO, HAM + SLAM, and HAM obtained from ITSG 2016 and ITSG 2018 from 20 to 120 days

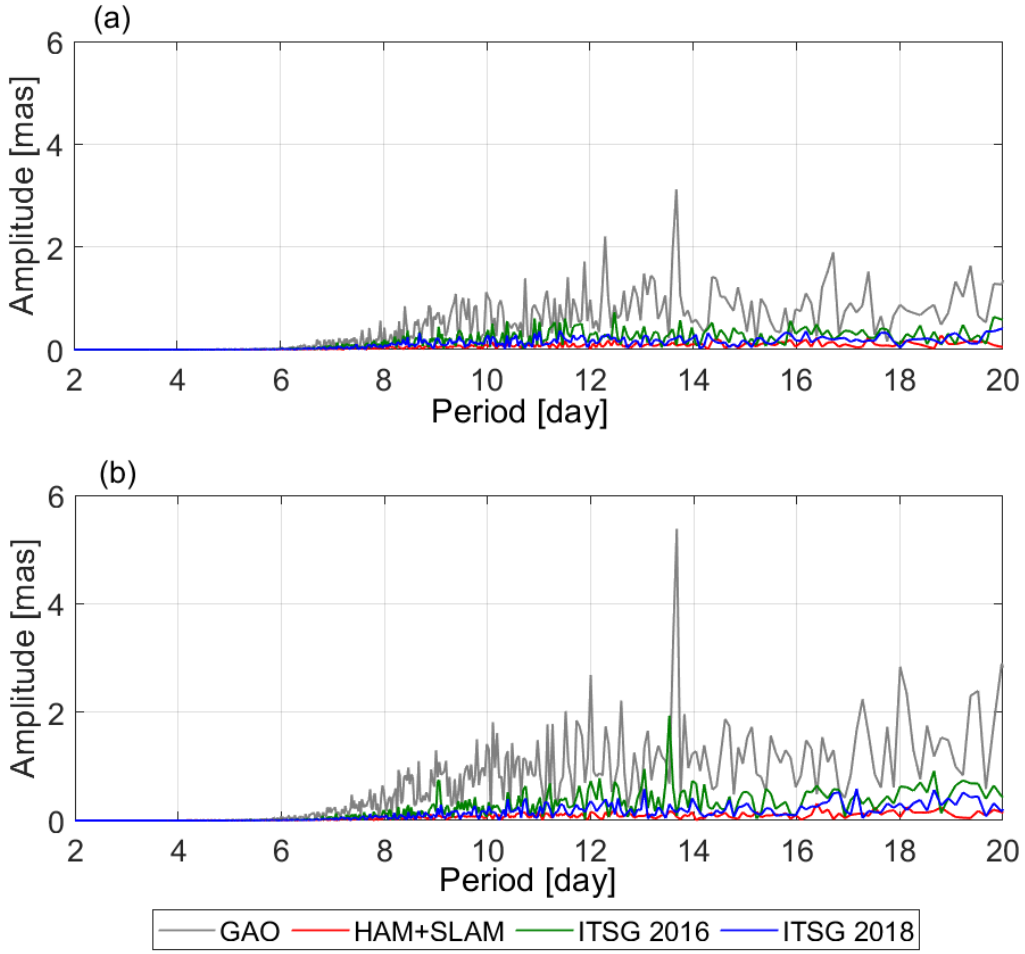


**Figure 4.** Comparison of (a) $\chi_1$ and (b) $\chi_2$ amplitude spectra series of GAO, HAM + SLAM, and HAM obtained from ITSG 2016 and ITSG 2018 from 2 to 20 days

### 4.3. Validation of series

In this section, we evaluate the ITSG-based HAM series and the HAM + SLAM series by analyzing RMSE, $Var_{exp}$, and correlations. These statistical indicators allow intercomparison of the time series and will help determine the similarities between the ITSG 2016-based series, ITSG 2018-based series, or the HAM + SLAM series and the GAO reference series.

The RMSE values of ITSG 2016-based series, ITSG 2018-based series, and HAM + SLAM series are shown in Figure 5. In $\chi_1$, the ITSG 2016-based series and ITSG 2018-based series have the same RMSE value (13.0 mas). Moreover, HAM + SLAM has an RMSE of 13.7 mas, which is slightly higher than for the ITSG-based series. In $\chi_2$, the RMSE values are higher and have a wider range than in $\chi_1$. The lowest value is RMSE of ITSG 2016-based series (19.4 mas) and the highest is RMSE of HAM + SLAM series (21.6 mas), which is the same as in $\chi_1$.

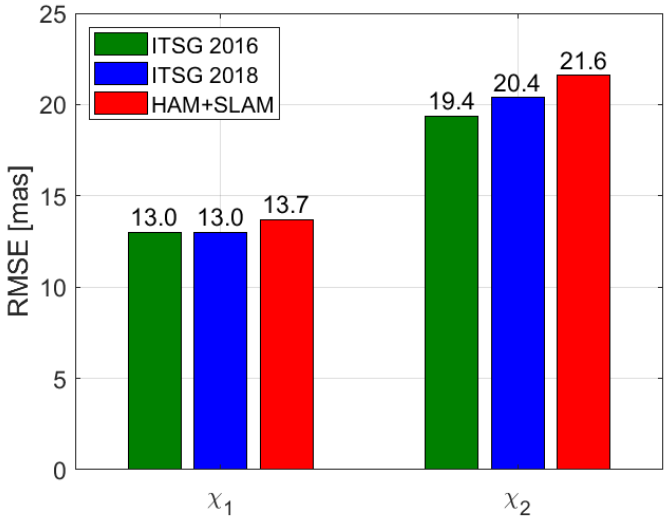


**Figure 5.** RMSEs of ITSG 2016-based series, ITSG 2018-based series, and HAM + SLAM calculated using GAO as the reference series. The exact RMSE values are given above the bars for each series.

All $Var_{exp}$ values are shown in Figure 6. In $\chi_1$, ITSG 2016 and ITSG 2018 have $Var_{exp}$ of 10% and HAM + SLAM has an explained variance of 0%. In $\chi_2$, the explained variance values of all series are highly variable. ITSG 2016 has the highest variance (21%), whereas ITSG 2018 has a lower explained variance (12%). HAM + SLAM has the lowest explained variance (1%), which is also found for $\chi_1$.

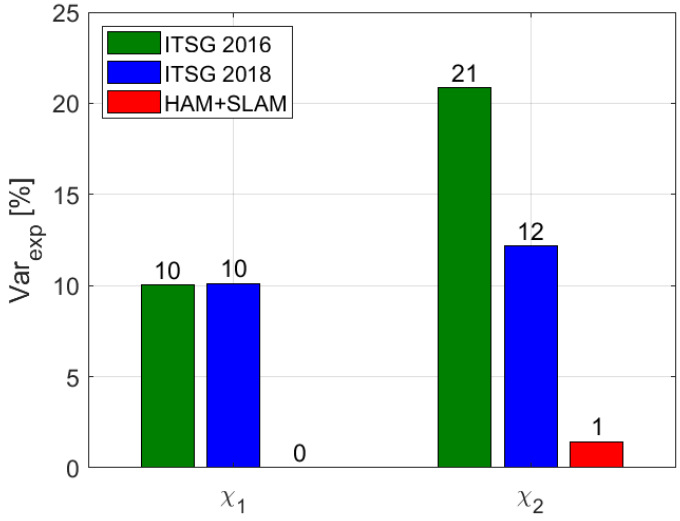


**Figure 6.** $Var_{exp}$ of ITSG 2016-based series, ITSG 2018-based series, and HAM + SLAM calculated using GAO as the reference series. The exact explained variance values are given above the bars for each series.

The final part of the analysis considers the correlation between all considered series. Correlations of ITSG-based series with reference series are statistically significant (the critical value of the correlation coefficient for 100 independent points is 0.17, and in our case, there are 500 independent points).

Figure 7 shows the calculated correlations for each time series. The ITSG-based series are better correlated with GAO in $\chi_2$ than in $\chi_1$, a result which is similar to previous studies

(Seoane et al., 2011; Chen et al., 2012; Wińska et al., 2017). If we compare the correlation coefficients of the ITSG-based series and the HAM + SLAM series with GAO, we observe a stronger correlation for the ITSG-based series. For $\chi_1$ (Figure 7a), the series have the following correlation coefficients: ITSG 2016, 0.35; ITSG 2018, 0.35; and HAM + SLAM, 0.07. For $\chi_2$ (Figure 7b), the series have the following correlation coefficients: ITSG 2016, 0.51; ITSG 2018, 0.41; and HAM + SLAM, 0.12. The correlations between ITSG-based series and GAO are similar for $\chi_1$; however, ITSG 2016 is better correlated with GAO than ITSG 2018 for $\chi_2$.

The advantage of ITSG 2016 over ITSG 2018 in $\chi_1$ may be due to the difference in the versions of the AOD1B models. The AOD1B RL05 model was used in ITSG 2016 and the AOD1B RL06 model in ITSG 2018. Compared to AOD1B RL05, changes such as increased spatial and temporal resolution, changing the ocean model from the Ocean Model for Circulation and Tides (OMCT; Dobslaw et al., 2013) to MPIOM (Jungclaus et al., 2013), and improved long-term consistency (Dobslaw et al., 2017a, b) have been made in AOD1B RL06. The correlations we examined after swapping AOD1B releases in the ITSG series may indicate better consistency of AOD1B RL05 with GAO compared to AOD1B RL06 (Table A1).

On comparing the ITSG-based series with HAM + SLAM, it is clear that ITSG 2018 is better correlated with HAM + SLAM than ITSG 2016 (Figure 7). The correlation values for $\chi_1$ (Figure 7a) are 0.24 for ITSG 2016 and 0.36 for ITSG 2018. The correlation values for $\chi_2$ (Figure 7b) are 0.25 for ITSG 2016 and 0.33 for ITSG 2018. There are no significant differences between $\chi_1$ and $\chi_2$ within each series, with values of 0.24 and 0.25 for $\chi_1$, and $\chi_2$, respectively, for ITSG 2016, and values of 0.36 and 0.33 for $\chi_1$ and $\chi_2$, respectively, for ITSG 2018.

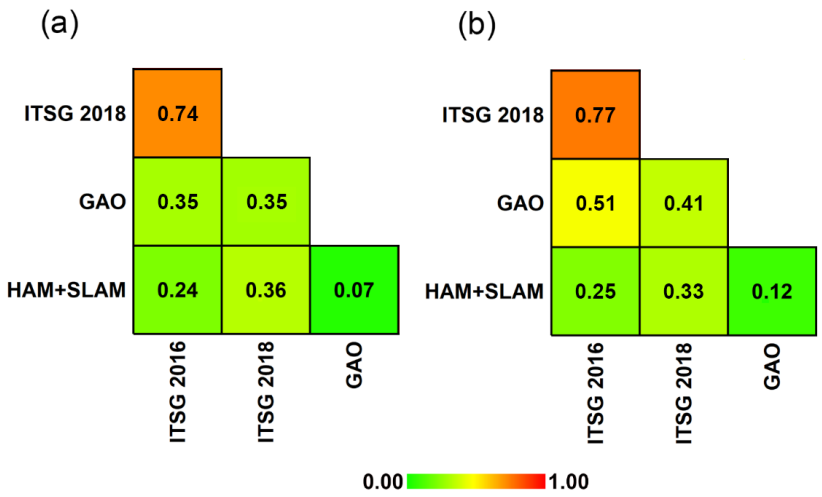


**Figure 7.** Correlations between ITSG 2016-based series, ITSG 2018-based series, GAO, and HAM + SLAM in (a) $\chi_1$ and (b) $\chi_2$

## 5. DISCUSSION AND SUMMARY

The main aim of this study was to evaluate the usefulness of ITSG daily gravity field models in the determination of HAM at nonseasonal time scales, which allows oscillations to be determined with higher frequencies than the more commonly used monthly data. A comparison was made with the hydrological signal in the PM excitation (GAO) and HAM + SLAM excitation series obtained from the LSDM hydrological model.

Determination of oscillations with higher frequencies provided an opportunity to investigate the existence of a sub-monthly signal in the HAM data. The results are promising, but not entirely satisfactory. Although ITSG-based HAM series have several times smaller amplitudes than GAO, they are still higher than HAM + SLAM obtained from LSDM. Analysis of amplitude spectra for oscillations with periods between 2 and 120 days showed that the ITSG-based HAM series, despite smaller amplitudes, have several common peaks with GAO. Of special note is the joint peak visible for ITSG 2016-based HAM and GAO around 14 days, which may be caused by the Earth's tides.

Our study showed that in the case of the $\chi_2$ component determined from ITSG-2018, deterioration in compliance was observed with GAO compared with the ITSG-2016-based series (lower correlation, lower relative explained variance, and higher RMSE). These differences might result from changes in processing between the ITSG 2016 and ITSG 2018 models.

The fact that the correspondence with GAO is higher after using the previous ITSG release (ITSG 2016) is a little unexpected. One of the factors why the level of agreement with GAO changed after the transition from the old and the new ITSG solution may have been the use of different AOD1B releases in ITSG 2016 and ITSG 2018 to eliminate atmospheric and oceanic nontidal contributions. To deepen this issue, we removed AODB RL06 from ITSG 2016 (instead of AODB RL05) and AODB RL05 from ITSG 2018 (instead of AODB RL06) and computed correlations with GAO (Table 3). It turned out that changing the AOD1B product had no noticeable effect on the correlations for $\chi_1$, but it affected the $\chi_2$ correlations to a greater extent. What is interesting, the change of AOD1B data from new to old in ITSG 2018 improved correlation coefficients with GAO, while the change of AOD1B data from old to new in ITSG 2016 worsened correlation coefficients with GAO. The ITSG 2018-based series with the AOD1B RL05 application appeared to achieve the highest correlation with GAO of all the series in $\chi_2$. It is a little puzzling that using the more recent AOD1B data does not provide improved consistency with GAO. Nevertheless, it should be kept in mind that in our study, we analyzed de-seasoned series, which were additionally filtered with the Butterworth filter to isolate oscillations with periods between 4 and 120 days. Therefore, this conclusion may not be valid for shorter oscillations as AOD1B data were originally processed in 3- and 6-h temporal resolution.

**Table 3.** Correlation coefficients between GAO and ITSG-based HAM series computed from ITSG 2016, ITSG 2018, ITSG 2016 with changed AOD1B data (AOD1B RL06 instead of RL05), and ITSG 2018 with changed AOD1B data (AOD1B RL05 instead of RL06)

| | **ITSG 2016** | **ITSG 2016 RL06** | **ITSG 2018** | **ITSG 2018 RL05** |
|---|---|---|---|---|
| $\chi_1$ | 0.35 | 0.31 | 0.35 | 0.32 |
| $\chi_2$ | 0.51 | 0.30 | 0.41 | 0.56 |

## 6. CONCLUSIONS

In conclusion, it can be stated that daily GRACE solutions provided by ITSG can be useful in determination of HAM at nonseasonal time scales. Although they do not ensure full compliance with GAO, their use is a much better alternative than the usage of hydrological models.

The correlations between ITSG-based HAM series and GAO are statistically significant and higher than between HAM + SLAM and GAO. The ITSG-based series have a correlation of

the same value in $\chi_1$ (0.35). In $\chi_2$, the ITSG 2016-based series has a higher correlation with GAO than the ITSG 2018-based series (0.51 and 0.41, respectively).

This study showed that the GAO series have the largest amplitudes and the highest STD (13.71 mas for $\chi_1$ and 21.76 mas for $\chi_2$) of all series, while the HAM + SLAM series have the smallest amplitudes and the lowest STD (1.99 mas for $\chi_1$ and 2.24 mas for $\chi_2$). The ITSG-based series have smaller amplitudes than GAO, but larger amplitudes than HAM + SLAM. The STD analysis showed that the ITSG 2016-based series is closer to GAO (5.48 mas for $\chi_1$ and 7.28 mas for $\chi_2$) than the ITSG 2018-based series (3.90 mas for $\chi_1$ and 5.05 mas for $\chi_2$).

In general, agreement between ITSG-based HAM and GAO, expressed by the higher correlation coefficient, lower RMSE, and higher $Var_{exp}$, is better in $\chi_2$ than in $\chi_1$, which is consistent with the findings from other studies (Göttl et al., 2018; Nastula et al., 2019; Seoane et al., 2011).

It should be recalled that, although GRACE was operational between 2002 and 2017, our study focused on analysis for the period between 2004 and 2011. This was because some gaps in GRACE data are present at the beginning and at the end of the mission, which also affect the daily solutions.

Because ITSG daily gravity field models (ITSG 2016 and ITSG 2018) can be useful to determine the equatorial components ($\chi_1$ and $\chi_2$) of HAM at nonseasonal time scales, studies exploiting GRACE data for interpretation of PM excitation should also be continued with inclusion of data from the mission successor, GRACE Follow-On.

**Acknowledgment.** The work of J. Śliwińska is financed by the National Science Center, Poland (NCN), grant number 2018/31/N/ST10/00209.

## REFERENCES

Bizouard, C. (2020). *Geophysical Modelling of the Polar Motion. In Geophysical Modelling of the Polar Motion*. https://doi.org/10.1515/9783110298093

Brzeziński, A. (1992). *Polar motion excitation by variations of the effective angular momentum function: considerations concerning deconvolution problem*. Manuscr. Geod., 17(1), 3–20.

Brzeziński, A., Nastula, J., & Kołaczek, B. (2009). Seasonal excitation of polar motion estimated from recent geophysical models and observations. *Journal of Geodynamics*, 48(3–5), 235–240. https://doi.org/10.1016/J.JOG.2009.09.021

Chen, J., Wilson, C., Chao, B., Shum, C. K., & Tapley, B. (2000). Hydrologic and oceanic excitations to polar motion and length-of-day variation. *Geophysical Journal International*, 141, 149–156. https://doi.org/10.1046/j.1365-246X.2000.00069.x

Chen, J. L., & Wilson, C. R. (2005). Hydrological excitations of polar motion, 1993–2002. *Geophysical Journal International*, 160(3), 833–839. https://doi.org/10.1111/j.1365-246X.2005.02522.x

Chen, J. L., Wilson, C. R., & Zhou, Y. H. (2012). Seasonal excitation of polar motion. *Journal of Geodynamics*, 62, 8–15. https://doi.org/10.1016/J.JOG.2011.12.002

Dill, R. (2008). Hydrological model LSDM for operational Earth rotation and gravity field variations. *Scientific Technical Report*. https://doi.org/11.2312/GFZ.b103-08095

Dobslaw, H., Dill, R., Grötzsch, A., Brzeziński, A., & Thomas, M. (2010). Seasonal polar motion excitation from numerical models of atmosphere, ocean, and continental hydrosphere.

*Journal of Geophysical Research: Solid Earth*, 115(B10). https://doi.org/https://doi.org/10.1029/2009JB007127

Dobslaw, H., Flechtner, F., Bergmann-Wolf, I., Dahle, C., Dill, R., Esselborn, S., Sasgen, I., & Thomas, M. (2013). Simulating high-frequency atmosphere-ocean mass variability for dealiasing of satellite gravity observations: AOD1B RL05. *Journal of Geophysical Research: Oceans*, 118(7), 3704–3711. https://doi.org/https://doi.org/10.1002/jgrc.20271

Dobslaw, H., Bergmann-Wolf, I., Dill, R., Poropat, L., Flechtner, F. (2017a) *Product description document for AOD1B release 06*. Technical report GRACE, 327–750. Available online: Ftp://isdcftp.gfz-potsdam.de/grace/DOCUMENTS/Level-1/GRACE_AOD1B_Product_Description_Document_for_RL06.pdf (accessed on 24.05.2023)

Dobslaw, H., Bergmann-Wolf, I., Dill, R., Poropat, L., Thomas, M., Dahle, C., Esselborn, S., König, R., & Flechtner, F. (2017b). A new high-resolution model of non-tidal atmosphere and ocean mass variability for de-aliasing of satellite gravity observations: AOD1B RL06. *Geophysical Journal International*, 211, 263–269. https://doi.org/10.1093/GJI/GGX302

Dobslaw, H., & Dill, R. (2018). Predicting Earth orientation changes from global forecasts of atmosphere-hydrosphere dynamics. *Advances in Space Research*, 61(4), 1047–1054. https://doi.org/https://doi.org/10.1016/j.asr.2017.11.044

Göttl, F., Schmidt, M., & Seitz, F. (2018). Mass-related excitation of polar motion: an assessment of the new RL06 GRACE gravity field models. *Earth, Planets and Space*, 70(1), 195. https://doi.org/10.1186/s40623-018-0968-4

Gross, R. (2015). *Theory of Earth Rotation Variations*. https://doi.org/10.1007/1345_2015_13

Jin, S., Chambers, D. P., & Tapley, B. D. (2010). Hydrological and oceanic effects on polar motion from GRACE and models. *Journal of Geophysical Research: Solid Earth*, 115(B2). https://doi.org/10.1029/2009JB006635

Jungclaus, J. H., Fischer, N., Haak, H., Lohmann, K., Marotzke, J., Matei, D., Mikolajewicz, U., Notz, D., & von Storch, J. S. (2013). Characteristics of the ocean simulations in the Max Planck Institute Ocean Model (MPIOM) the ocean component of the MPI-Earth system model. *Journal of Advances in Modeling Earth Systems*, 5(2), 422–446. https://doi.org/https://doi.org/10.1002/jame.20023

Kurtenbach, E., Eicker, A., Mayer-Gürr, T., Holschneider, M., Hayn, M., Fuhrmann, M., & Kusche, J. (2012). Improved daily GRACE gravity field solutions using a Kalman smoother. *Journal of Geodynamics*, 59–60, 39–48. https://doi.org/10.1016/J.JOG.2012.02.006

Lambeck, K. (1980). *The earth's variable rotation: geophysical causes and consequences. The Earth's Variable Rotation: Geophysical Causes and Consequences*. https://doi.org/10.1016/0031-9201(81)90054-6

Mayer-Gürr, T., Behzadpour, S., Ellmer, M., Kvas, A., Klinger, B., Zehentner, N. (2016). *ITSG-Grace2016-Monthly and Daily Gravity Field Solutions from GRACE*. GFZ Data Services. Available online: http://dataservices.gfz-potsdam.de/icgem/showshort.php?id=escidoc:1697893

Mayer-Gürr, T., Behzadpour, S., Ellmer, M., Kvas, A., Klinger, B., Strasser, S., Zehentner, N. (2018). *ITSG-Grace2018-Monthly, Daily and Static Gravity Field Solutions from GRACE*. GFZ Data Services. Available online: http://dataservices.gfz-potsdam.de/icgem/showshort.php?id=escidoc:3600910

Meyrath, T., & van Dam, T. (2016). A comparison of interannual hydrological polar motion excitation from GRACE and geodetic observations. *Journal of Geodynamics*, 99. https://doi.org/10.1016/j.jog.2016.03.011

Munk, W. H., & MacDonald, G. J. F. (1960). *The rotation of the earth; a geophysical discussion*. Cambridge [Eng.] University Press.

Nastula, J., Wińska, M., Śliwińska, J., & Salstein, D. (2019). Hydrological signals in polar motion excitation – Evidence after fifteen years of the GRACE mission. *Journal of Geodynamics*, 124, 119–132. https://doi.org/10.1016/J.JOG.2019.01.014

Seoane, L., Nastula, J., Bizouard, C., & Gambis, D. (2011). Hydrological Excitation of Polar Motion Derived from GRACE Gravity Field Solutions. *International Journal of Geophysics*, 2011, 174396. https://doi.org/10.1155/2011/174396

Sidorenkov, N. (2009). *The Interaction Between Earth's Rotation and Geophysical Processes*. The Interaction Between Earth's Rotation and Geophysical Processes by Nikolay S. Sidorenkov. Wiley, 2009. ISBN: 978-3-527-40875-7. https://doi.org/10.1002/9783527627721

Śliwińska, J., Nastula, J., Dobslaw, H., & Dill, R. (2020). Evaluating Gravimetric Polar Motion Excitation Estimates from the RL06 GRACE Monthly-Mean Gravity Field Models. *Remote Sensing*, 12(6). https://doi.org/10.3390/rs12060930

Śliwińska, J., Winska, M., & Nastula, J. (2022). Exploiting the Combined GRACE/GRACE-FO Solutions to Determine Gravimetric Excitations of Polar Motion. *Remote Sensing*, 14, 6292. https://doi.org/10.3390/rs14246292

Tapley, B. D., Bettadpur, S., Watkins, M., & Reigber, C. (2004). The gravity recovery and climate experiment: Mission overview and early results. *Geophysical Research Letters*, 31(9). https://doi.org/10.1029/2004GL019920

Winska, M., Nastula, J., & Salstein, D. (2017). Hydrological excitation of polar motion by different variables from the GLDAS models. *Journal of Geodesy*, 91(12), 1461–1473. https://doi.org/10.1007/s00190-017-1036-8

***Received:*** *2023-03-13*

***Reviewed:*** *2023-04-24 (A. Bhardwaj); 2023-04-26 (H. Lecomte)*

***Accepted:*** *2023-07-10*

**APPENDIX**

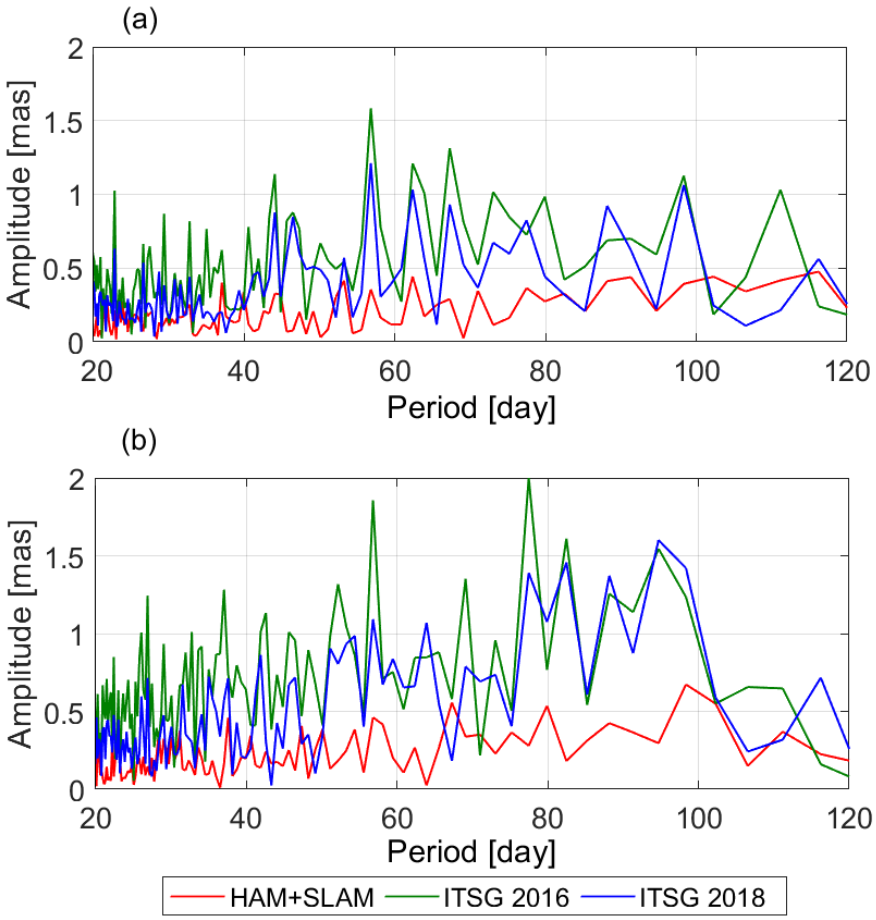


**Figure A1.** Comparison of (a) $\chi_1$ and (b) $\chi_2$ amplitude spectra series of HAM + SLAM and HAM obtained from ITSG 2016 and ITSG 2018 from 2 to 120 days

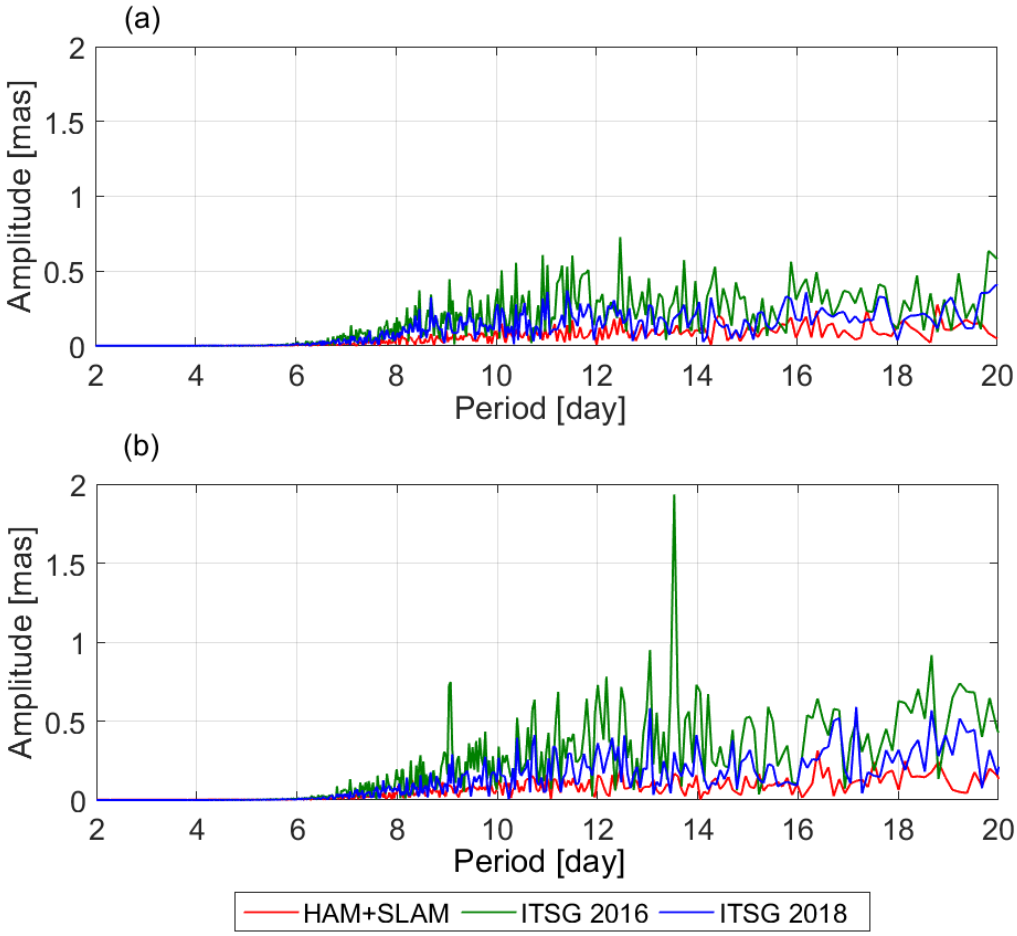


**Figure A2.** Comparison of (a) $\chi_1$ and (b) $\chi_2$ amplitude spectra series of HAM + SLAM and HAM obtained from ITSG 2016 and ITSG 2018 from 2 to 20 days